Preliminary Report: Enhanced Passive Seismic Characterization of High Priority Salt Jugs in Hutchinson, Kansas

Julian Ivanov, Richard D. Miller, Shelby L. Peterie,
J. Tyler Schwenk, J. Jordan Nolan, Brett Bennett,
Brett Wedel, Joe Anderson, Jerry Chandler,
and Shawn Green

Kansas Geological Survey
1930 Constant Avenue
Lawrence, KS 66047

Revised Preliminary Report to

Ed Lindgren and Pete Burton
Burns & McDonnell Engineering Company
9400 Ward Parkway
Kansas City, MO 64114
(816) 822-3138

Open-File Report 2018-2 June 7, 2013

Preliminary Report: Enhanced Passive-Seismic Characterization of High-Priority Salt Jugs in Hutchinson, Kansas

Executive Summary

This applied research project correlated measured shear-wave velocities with the condition of dissolution voids and the physical properties of the overburden at selected locations on VigIndustries legacy solution mining property in Hutchinson, Kansas. Shear-wave velocities were estimated from passive surface-wave data acquired along eight profiles that intersected 13 wells. Two of these 13 wells had been the target of a previous seismic investigation completed in 2008. As a result of that 2008 study it was determined that the integrity of the overlying strata could be reasonably estimated using shear-wave seismic imaging. The 2008 study quantified the effectiveness of shear-wave velocity to estimate local stress above voids of the size and depth prevalent at the VigIndustries site in Hutchinson. For this study, multichannel analysis of surface waves (MASW) was used to estimate the shear-wave velocity, map stratigraphic contacts from as near the top of the "three finger" dolomite as possible to the ground surface, appraise the apparent integrity of void roofs, and prioritize voids suspected to have the potential for vertical migration and eventual surface collapse.

Passive MASW data were acquired along several profiles during three surveys at two locations near the Irsik & Doll elevators. Five lines and a surface grid of receivers targeted key wells in proximity to the elevator during the first survey. During the second survey, two lines and a surface grid of receivers were deployed for additional, focused investigation along two lines acquired during the first survey. A third line that was occupied during the second trip targeted key wells along William Street with the intent of correlating findings with previous surveys in that area. During the third survey trip, two lines and a surface grid of receivers were deployed to increase spatial sampling and signal-to-noise ratio of data acquired during previous surveys and to improve the confidence of interpretations at wells 2A and 4B. For all surveys reported here, surface waves with frequencies as low as 4 Hz were recorded from an average maximum depth of investigation of around 70 m, and in some places as deep as 100 m.

With shear-wave velocity being a function of the shear modulus and density, stress on overburden rocks (shear modulus) can be quantified using shear wave velocity values. Therefore, local increases in shear velocity have been attributed to elevated stress resulting from changes in the overburden roof load. With each failure of a void's roof (the roof as defined by the tensional dome) the shear velocity will decrease consistent with the resultant reduction in overburden stress. Stress (shear modulus), and therefore shear velocity, increases over time as the stress regime at and around the void's roof increases. These increases are generally due to fatigue and minor spalling. Markedly lower shear velocity zones, relative to surrounding rocks, are generally associated with collapse features. The migration path of voids can normally be characterized by low velocity chimney features originating at the original dissolution jug and extending to the bedrock surface or, in the case of subcritical jugs (insufficient volume to accommodate all the spall material produced between original jug top and bedrock surface), the vertical migration of a collapse feature will be arrested by bulking prior to reaching the bedrock surface.

Shear velocities in the majority of the areas studied are characteristics of a normal stress regime and natural geologic variation. A tensional dome observed in the bedrock south of the

grain elevator at well 5B suggests elevated stress, potentially a byproduct of an undersupported roof. Although the shear velocity of this feature is anomalous, it represents a relatively small increase and a key indicator of the fidelity of the method. Expectations based on the character and amplitude of the anomaly are that the unsupported roof of the void at 5B is small, flat, and located at or just above the salt/shale contact. The anomaly is not dramatic enough to imply rapid migration or impending collapse. Equally significant, the observed gentle westward velocity gradient and increased depth of surface-wave penetration near wells 4B and 2A are interpreted to be consistent with natural geologic variation for this site.

A localized off-well velocity increase observed on two lines approximately 40 m south of well 3B is a subtle indicator of a potential gallery style anomaly. As well, velocities observed at well 52 suggest minimally lower stress, indicative of previous/possible recent collapse and a current stable roof. Velocities observed at well 53 are suggestive of slightly increased stress. Based on *a priori* information from sonar surveys, the roof of this void has likely undergone incremental failure, relieving stress that would have been present at the time of the sonar survey. Currently, it is likely the void has a domed roof that is closer to the ground surface and is distributing stress more uniformly across a wider surface area, representing no threat of imminent vertical migration and collapse. Results at wells 52 and 53 are relatively consistent with the previous seismic study, confirming that passive MASW is an effective tool for evaluating stress above voids of this size and depth.

Introduction

Material properties (specifically strength and stress accumulations) measured as a function of depth above abandoned salt jugs in Hutchinson, Kansas, appear related to the mobility and upward migration potential of these jugs. Localized escalation in stress (as indicated by increased shear-wave velocity) above subterranean voids is one indicator of an increased potential for roof failure and void migration (Eberhart-Phillips et al., 1989; Dvorkin et al., 1996; Khaksar et al., 1999; Sayers, 2004). Previous studies, using both active and passive seismic wavefield characteristics, suggest perturbations in the shear-wave velocity field immediately above voids can be correlated to characteristics of the unsupported roof spans of salt jugs in this area (Sloan et al., 2010).

The strength of individual rock layers can be qualitatively described in terms of stiffness/rigidity and empirically estimated from relative comparisons of shear-wave velocity measurements. Shear-wave velocity is directly proportional to stress and inversely related to non-elastic strain. Since the shear-wave velocity of earth materials changes when stress and any associated elastic strain on those materials becomes "large," it is reasonable to suggest load-bearing roof rock above mines or dissolution voids may experience elevated shear-wave velocities due to loading between pillars, or, in the case of voids, loading between supporting side walls. This localized increase in shear velocity is not related to increased strength, but increased load as defined by Young's Modulus. High-velocity shear-wave "halos" encompassing low-velocity anomalies are suggested to be key indicators of near-term roof failure. All these phenomena have been observed at this Hutchinson, Kansas, site at depths greater than 30 m below the bedrock surface.

Previous active seismic reflection experiments at this site have detected areas with elevated shear-wave velocity likely indicative of an imminent risk for vertical migration of specific salt jugs (Sloan et al., 2010). The lack of necessary ultra low-frequency surface waves

in the recorded wavefield have negated attempts to use active source MASW to estimate shear velocity in the lithified rocks near the top of bedrock (Miller et al., 2009). Uncontrolled local industrial and transportation activities represent sound sources that have produced the necessary low frequencies and, when recorded and processed using passive methods, have extended the imaging depth to more than 60 m (Miller, 2011).

Passive surface-wave recording allows random sources of seismic energy (trains, manufacturing facilities, heavy vehicles on roadways, processing plants, heavy construction equipment, etc.), considered noise on active surveys, to be recorded so that data processing enhancements and specialized processing methods can be used to calculate the 1-D shear wave velocity function. Key to this method is the ability to estimate shear-wave velocities to depths double or more than possible with standard active sources at a particular site (Park et al., 2004). To evaluate the feasibility of the method at this site, two well locations (well 25/40, with void roof well into shale overburden; and well 94, with void roof down in salt) were selected with theoretically different stress regimes above known voids. Results of that feasibility study at wells 25/40 and 94 suggest the method is effective in predicting jugs with heightened risk for upward migration (Miller, 2011).

Seismograms recorded with train source energy and edited based on computer-aligned 2-D receiver grids possessed surface-wave frequencies low enough to effectively sample depths in excess of 60 m (Miller, 2011). Computer automated routines evaluated a wide range of possible 2-D receiver sub-grid orientations (subsets of the entire recording array), recommending a grid orientation and configuration that was tuned to produce the best dispersion curve (Miller, 2011). Some wells targeted for study are located in areas not amenable to 2-D grids of receivers, making it impractical to use the same approach for all wells. For this study, a single 2-D grid was deployed to evaluate and optimize source alignment with respect to each 1-D seismic line to effectively identify void roofs with elevated stress and therefore an elevated risk of vertical migration.

Geologic and Geophysical Setting

The Permian Hutchinson Salt Member occurs in central Kansas, northwestern Oklahoma, and the northeastern portion of the Texas Panhandle, and is prone to and has an extensive history of dissolution and formation of sinkholes (Figure 1). In Kansas, the Hutchinson Salt Member possesses an average net thickness of 75 m and reaches a maximum of more than 150 m in the southern part of the basin. Deposition occurring during fluctuating sea levels caused numerous halite beds, 0.2 to 3 m thick, to be formed interbedded with shale, minor anhydrite, and dolomite/magnesite. Individual salt beds may be continuous for only a few miles despite the remarkable lateral continuity of the salt as a whole (Walters, 1978).

The distribution and stratigraphy of the salt is well documented (Dellwig, 1963; Holdoway, 1978; Kulstad, 1959; Merriam, 1963). The salt reaches a maximum thickness in central Oklahoma and thins to depositional edges on the north and west, erosional subcrop on the east, and facies changes on the south. The increasing thickness toward the center of the salt bed is due to a combination of increased salt and more and thicker interbedded anhydrites. The Stone Corral Formation (a well documented seismic marker bed) overlies the salt throughout Kansas (McGuire and Miller, 1989). Directly above the salt at this site is a thick sequence of Permian shales.

The upper 760 m of rock at this site is Permian shales (Merriam, 1963). The Chase Group (top at 300 m deep), lower Wellington shales (top at 245 m deep), Hutchinson Salt (top at 120 m deep), upper Wellington shales (top at 75 m deep), and Ninnescah Shale (top at 25 m deep) make up the packets of reflecting events easily identifiable and segregated within the Permian portion of the section (Figure 2). Bedrock is defined as the top of the Ninnescah Shale with the unconsolidated Pliocene-Pleistocene Equus Beds making up the majority of the upper 30 m of sediment. Thickness of Quaternary alluvium that fills the stream valleys and paleosubsidence features goes from 0 to as much as 90 m, depending on the dimensions of the features.

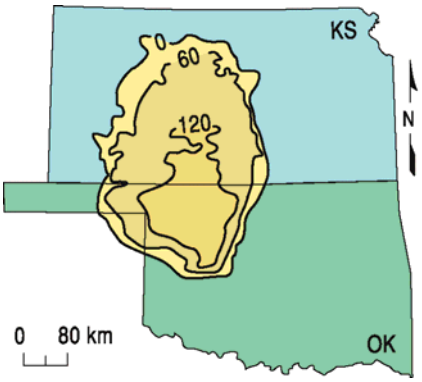

Figure 1. Approximate extent of salt formation, with contour intervals expressed in meters.

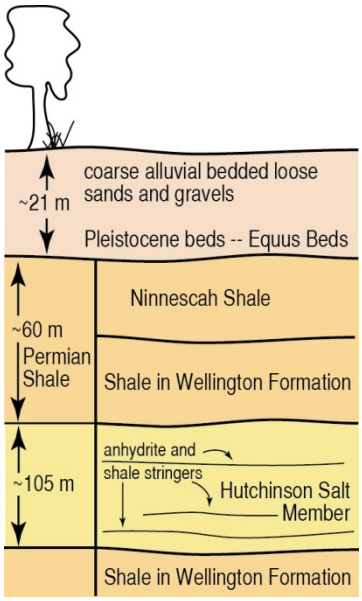

Figure 2. Generalized geology.

Recent dissolution of the salt and resulting subsidence of overlying sediments forming sinkholes has generally been associated with mining or saltwater disposal (Walters, 1978). Historically, these sinkholes can manifest themselves as a risk to surface infrastructure. The rate of surface subsidence can range from gradual to catastrophic. Subsidence features associated with salt removal (regardless of the method or catalyst) can have an impact on the geology and hydrology from the salt through the unlithified soils above bedrock. Natural sinkholes resulting from dissolution of the salt by localized leaching within natural flow systems that have been altered by structural features (such as faults and fractures) are not uncommon west of the main dissolution edge (Merriam and Mann, 1957).

Caprock and its characteristics are a very important component of any discussion concerning dissolution, subsidence, and formation of sinkholes. The Permian shales (Wellington and Ninnescah) that overlay the Hutchinson Salt Member are about 60 m thick in this area and are characterized as generally unstable when exposed to freshwater, being susceptible to sloughing and collapse (Swineford, 1955). These Permian shales tend to be red or reddish-brown and are commonly referred to as "red beds." Permian red beds are extremely impermeable to water and have therefore provided an excellent seal between the freshwaters of the Equus Beds and the extremely water-soluble Hutchinson Salt Member. The modern-day expanse and mere presence of the Hutchinson Salt is due to the protection from freshwater provided by these red beds.

Isolating the basal contact of the Wellington Formation provides key insights into the general strength of roof rock expected if dissolution-mined salt jugs (salt jugs are the cavities or voids in the salt—many times shaped like jugs—that form after salt has been dissolution mined in proximity to the wells) reach the top of the salt zone. Directly above the salt/shale contact is an approximately 6-m-thick dark-colored shale with joint and bedding cracks filled with red halite (Walters, 1978). Once unsaturated brine comes in contact with this shale layer, these red-halite-filled joints and bedding planes are rapidly leached, leaving an extremely structurally weak layer.

Study I: Irsik & Doll Elevators, August 2012

Field Layout and Data Acquisition

Prior to deployment, a bulldozer cleared the survey area to remove debris for optimum receiver coupling. To ensure the highest quality data, receivers were deployed during the day and train data were recorded at night when cultural and industrial noise was minimal to provide optimum signal-to-noise. Analysis of the previous seismic energy sources captured during passive recording at this site clearly indicated trains from a distance of 3 km or more away provided the best broad spectrum, low-frequency seismic energy (Miller, 2011). Because seismic energy with characteristics best suited for the purpose of this study may arrive when trains are at a distance greater than they can be detected by spotters, seismic records were recorded continuously during acquisition to ensure that optimum data were recorded.

Five lines and a surface grid of receivers were deployed over key wells near the Irsik & Doll elevators (Figure 3). Seismic receivers were single GeoSpace GS11D 4.5 Hz geophones. The seismic lines varied in length (Table 1), totaling more than 1.5 km with receivers spaced 3 m. The surface monitoring grid consisted of 144 receivers spaced at 5 m, configured to form four concentric expanding squares with 15, 35, 55, and 75 m sides. Data were recorded during two nights with a 400+ channel 24-bit Geometrics Geode distributed seismic system. Seismic

records were 32 s long with a 2 ms sampling interval. In total, 1105 seismic records equivalent to 28.8 GB of data were recorded.

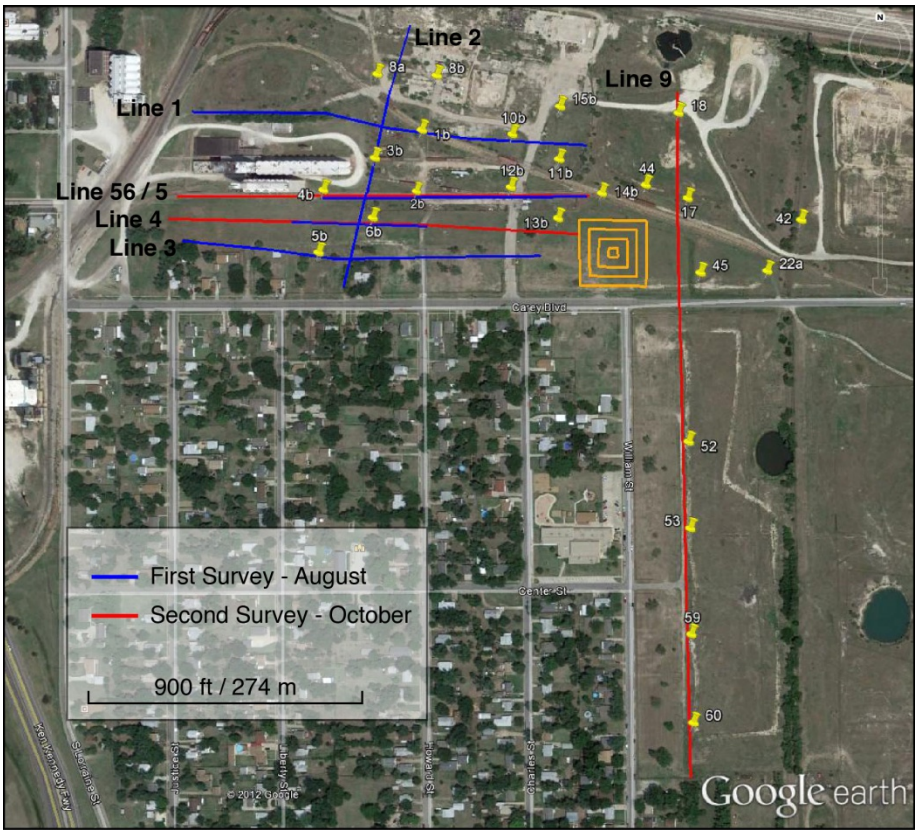

Figure 3. Aerial photo indicating GPS locations of seismic lines from the August survey (in blue), October survey (in red), 2D receiver grid used during both surveys (in orange), and locations of wells in the study area (yellow pins).

Table 1. Number of receivers and total line lengths for the 1-D seismic lines.

	line 1	line 2	line 3	line 4	line 56
number of receivers	144	96	126	48	96
total length (m)	429	285	375	141	285

Processing and Analysis

Data were processed using algorithms developed at KGS. The passive method used for this study is well published and provides good quality results at this site (Park et al., 2004). Unlike the previous study (Miller, 2011) where a surface grid of receivers and line of receivers were used principally with E/W trains along a range of offsets, this study used only 1-D spreads of receivers, trains from optimal distances, and trains properly aligned with the line orientations. This approach dramatically improves the accuracy of dispersion-curve analysis and minimizes the standard deviation.

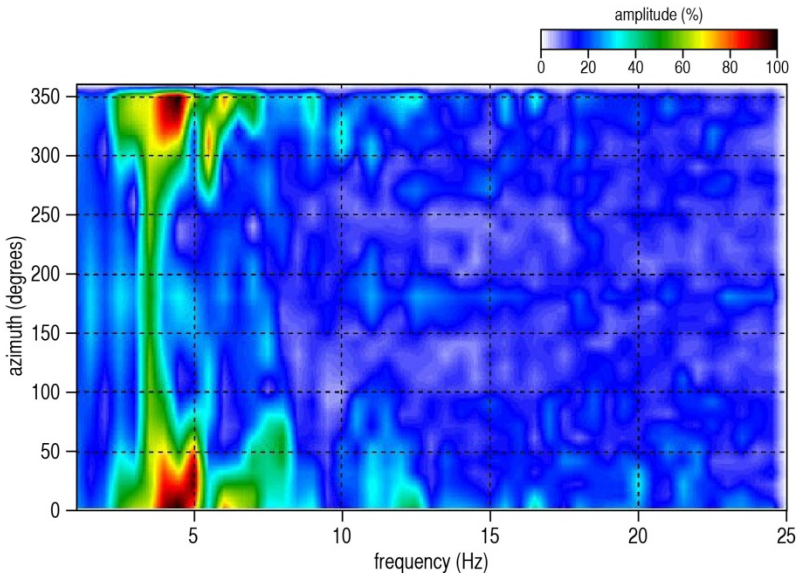

Figure 4. Azimuth plot indicating the direction of the dominant passive source energy (in degrees counterclockwise from east). Here, the dominant passive source energy is centered on 0°, due east.

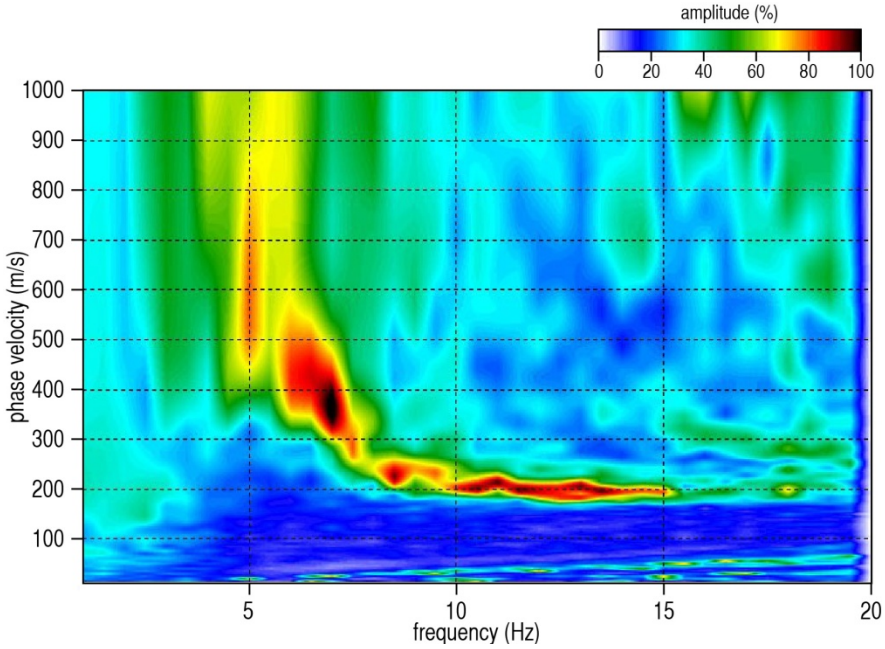

Figure 5. Representative overtone plot with high signal-to-noise ratio of the fundamental-mode Rayleigh wave.

For each line, the surface-wave amplitudes recorded by the surface grid were plotted as phase velocity versus frequency for a range of azimuths from 0 to 180 degrees with respect to the seismic line to determine which record had the best broadband, low frequency source with an azimuth near parallel to the line (Figure 4). The seismogram with optimum source characteristics was selected and divided into the shortest groups of receivers ("spread length") determined to provide overtone plots (phase velocity versus frequency) with high amplitude fundamental mode Rayleigh-wave energy and minimal higher-order surface-wave interference (Figure 5). For this study, 120 m spread lengths every 15 m were determined to provide optimal overtones and spatial sampling. Fundamental-mode dispersion curves were picked and inverted to obtain a 2-D section of shear-wave velocity (V_s) as a function of depth. The apparent velocity (v_{app}) is:

$$v_{app} = \frac{v_{act}}{(\cos\theta)} \tag{1}$$

where v_{act} is the actual seismic velocity and θ is the azimuth of the source with respect to the seismic line determined from the azimuth versus frequency plot. Thus, the increase in velocity (Δv) is:

$$\Delta v = \frac{1}{\cos\theta} - 1 \tag{2}$$

Equation 2 was used to calculate the increase in velocity due to the source azimuth for each line (Table 2).

Table 2. Directions of the passive seismic sources and the seismic lines (in degrees counterclockwise from east), the angle of the source with respect to the line (θ), and the percent increase in apparent velocity caused by oblique source orientations (Δv).

line	source orientation	line orientation	θ	Δv
1	10°	-5°	15°	4%
2	225°	255°	30°	15%
3	10°	-5°	15°	5%
4	0°	-1°	-1°	< 1%
56	10°	1°	9°	1%

Redundant processing was undertaken to verify the preliminary findings and validate the methods used. To confirm that the spatial sampling was adequate for characterizing shear-wave velocity at this site, the original line 3 data were reprocessed using 6 m spatial sampling and results were compared to the original processing. To confirm that velocity values were not source dependent, data acquired with a secondary, suboptimal train source were processed for line 3 and compared to results from the primary source.

Results and Interpretation

Line 1 is oriented in a nearly W-E direction and is located approximately 50 m north of the grain elevator. Velocities at the east end of line 1 are consistent with velocities from previous studies and with expectations for the geology at this site, which suggests a normal stress

regime (Figure 6). There is a gentle velocity gradient west of well 1B, and increased depth of surface-wave penetration between wells 1B and 2A. These characteristics are suggestive of natural geologic variation; however, additional data over well 2A is required to fill in and improve the dataset and enhance the interpretation.

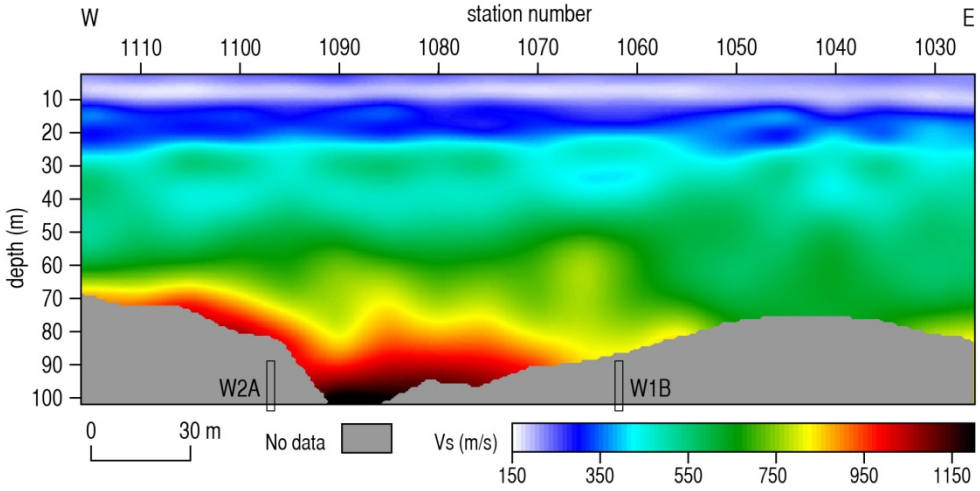

Figure 6. Final shear-wave velocity profile from Line 1 of the August survey. Approximate well locations are indicated at the bottom of the profile.

Line 2 is oriented NNE-SSW and is located approximately 20 m east of the elevator. A uniform 10-15% increase in velocity with respect to line 1 is expected for the source orientations of lines 1 and 2. Therefore, the slight increase in apparent velocity on line 2 is caused by the oblique source orientation, and the velocity structure at well 3B is suggestive of a normal stress regime (Figure 7).

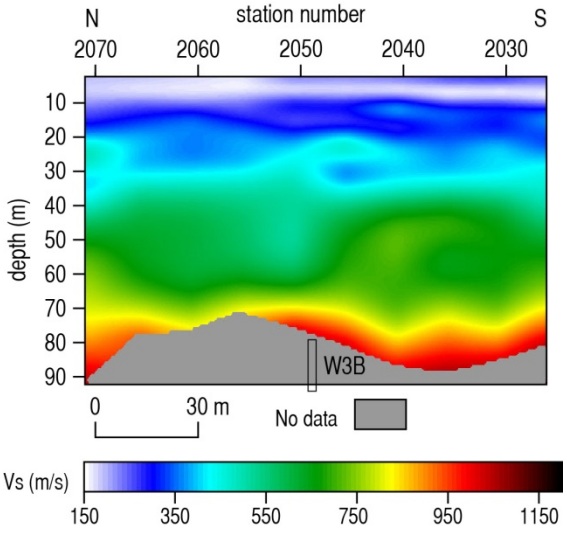

Figure 7. Final shear-wave velocity profile from Line 2 of the August survey. Approximate well locations are indicated at the bottom of the profile.

Line 3 is oriented W-E and is located approximately 60 m south of the elevator. In general, depths and velocities of stratigraphic units are consistent with those of line 1. However, a dome-shaped 15% velocity increase centered about well 5B is suggestive of elevated stress on the roof of a relatively small (<15 m) underlying void (Figure 8). The total size of the anomaly is approximately 30 m, suggesting a void top of <15 m.

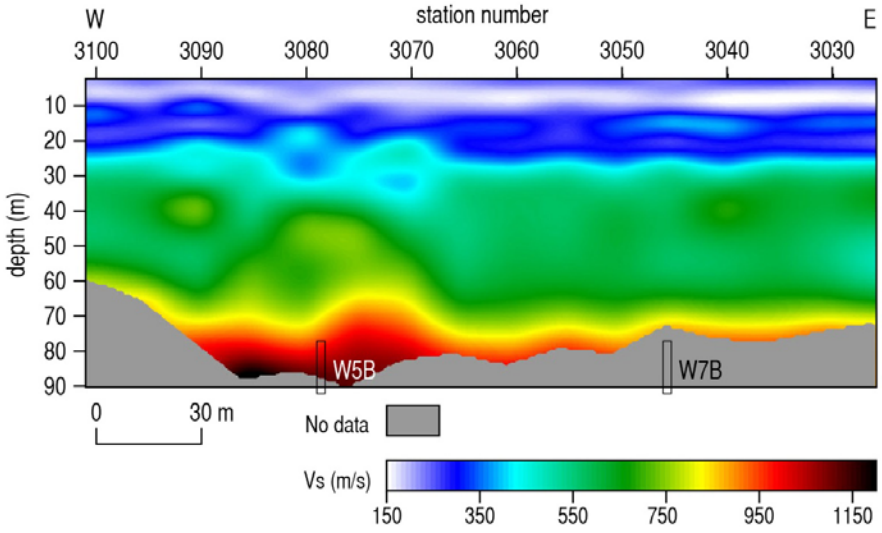

Figure 8. Final shear-wave velocity profile from Line 3 of the August survey. Approximate well locations are indicated at the bottom of the profile.

Lines 4 and 56 are oriented W-E and located 50 m and 25 m south of the elevator, respectively. Depths and velocities of stratigraphic units are consistent with lines 1 and 3. Increased depth of surface-wave penetration and velocity increase are observed on the west end of both profiles in the direction of well 4B (Figures 9 and 10). Although the velocity is anomalous, it is probably related to geologic variations, similar to the trend observed on Line 1, and/or end of the line effects. Additional data is required to fill in and improve the dataset and enhance the interpretation. Due to their proximity to the elevators and the potential to form a gallery with nearby well 5B, wells 4B and 6B were considered a priority for additional seismic investigation. The velocity profile over wells 2B and 12B appears to be indicative of a normal stress regime.

The velocity profile resulting from processing line 3 with denser spatial sampling (Figure 11) is, in general, consistent with the original profile. The depths, velocities, and overall structure of the major stratigraphic units are nearly identical. Apparent undulation of the "three finger" dolomite is caused by subtle variations in the inversion of the picked dispersion curves, a normal occurrence. Increased spatial sampling causes the subtle variations in the inversion to become more obvious. The wavelength of surface waves at this depth is approximately 140 m, too large to detect such small geologic undulations. Likewise, the gentle dip in the top of the dolomite beneath the top of the high velocity anomaly at well 5B is most likely a result of differences in the inversion caused by the increased velocity in the overlying bedrock. In general, the data suggest that the original spatial sampling (15 m) is sufficient to accurately characterize the general geology, shear wave velocity, and material strength at this site.

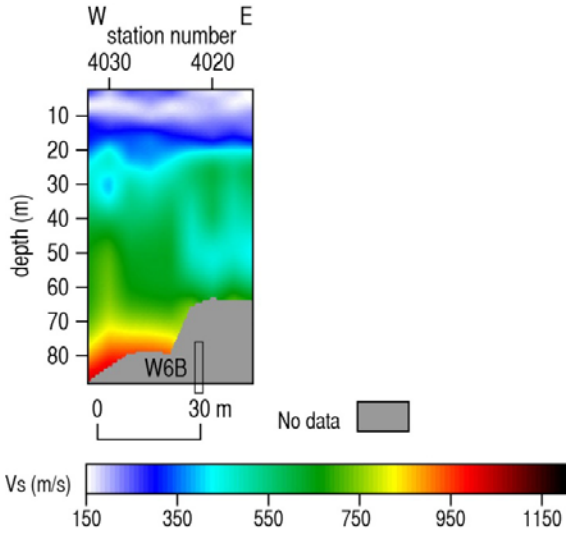

Figure 9. Final shear-wave velocity profile from Line 4 of the August survey. Approximate well locations are indicated at the bottom of the profile.

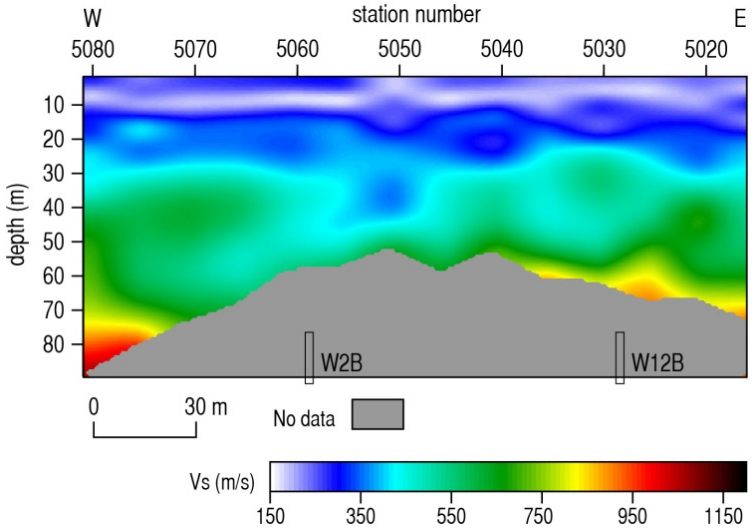

Figure 10. Final shear-wave velocity profile from Line 56 of the August survey. Approximate well locations are indicated at the bottom of the profile.

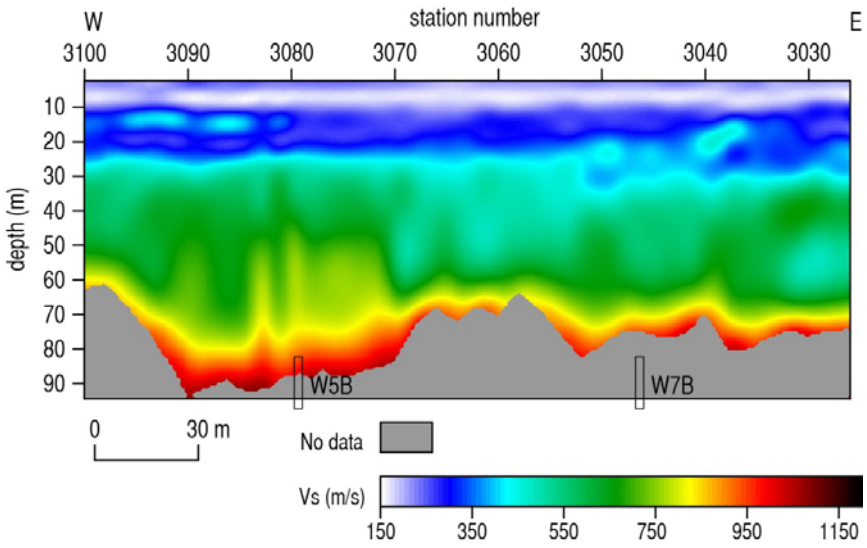

Figure 11. Shear-wave velocity profile from line 3 reprocessed with 60% denser spatial sampling.

Because this is a passive survey, the energy source is unpredictable and uncontrollable. The chance nature of the source affects the quality and usefulness of the recorded data. As expected, differences in the primary and secondary train events (distance, speed, length, weight, etc.) used to process line 3 resulted in slightly different velocity profiles. The profile produced using data from the secondary source (Figure 12) shows the same general velocity trend as the primary source (Figure 8). As expected, the suboptimal spectral characteristics recorded with the secondary source result in a less coherent high-velocity anomaly centered on well 5B, but nevertheless validate the original interpretation of results from the primary source.

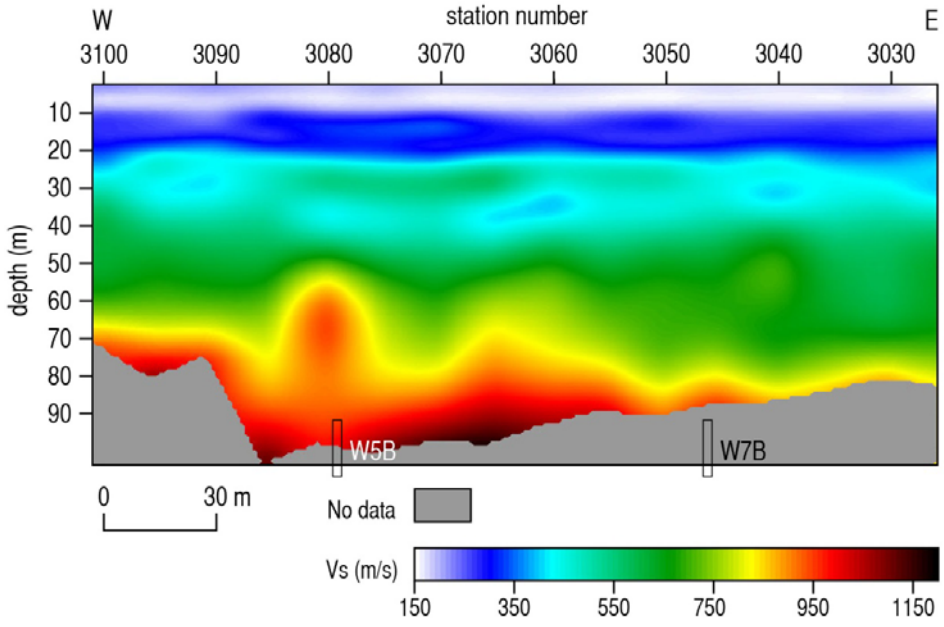

Figure 12. Shear-wave velocity profile from line 3 reprocessed with a secondary source.

Study II: William Street, Irsik & Doll follow-up, October 2012

Field Layout and Data Acquisition

A second survey was acquired to improve determination of the size and shape of anomalies near the Irsik & Doll elevators from the August 2012 dataset and investigate the series of wells located along William Street. Three lines and a surface grid of receivers were deployed in the study area (Figure 3). As in the previous survey, seismic receivers were single GeoSpace GS11D 4.5 Hz vertical geophones. The seismic lines varied in length (Table 3), totaling more than 1.5 km with receivers spaced 3 m. The surface monitoring grid was geospatially located and deployed at the same location as the grid from the previous study. Data were recorded during two nights with a 400+ channel 24-bit Geometrics Geode distributed seismic system. Seismic records were 32 s long with a 2 ms sampling interval. In total, 1014 seismic records equivalent to 24.8 GB of data were recorded.

Table 3. Number of receivers and total line lengths for the 1-D seismic lines.

	line 4	line 56	line 9
number of receivers	144	144	240
total length (m)	429	429	720

Processing and Analysis

Due to the variations in the characteristics of available energy sources (e.g., distance, speed, length, weight), the signal-to-noise ratio of recorded surface wave energy is less than the August 2012 survey, particularly at higher frequencies. Data were processed consistent with the previous survey, with additional advanced processing techniques (e.g., time window stacking, increased spread length) applied to sufficiently increase signal-to-noise and improve confidence in final results. The apparent velocity increase associated with source azimuth was less than 1% for the records that were processed (Table 4).

Table 4. Directions of the passive seismic sources and the seismic lines (in degrees counterclockwise from east), the angle of the source with respect to the line (θ), and the percent increase in apparent velocity caused by oblique source orientations (Δv).

line	source orientation	line orientation	θ	Δv
9	88°	91°	3°	< 1%
4	0°	358°	2°	< 1%
56	355°	1°	6°	< 1%

Results and Interpretation

Line 4 was deployed with a W-E orientation near line 4 from the August 2012 study. Depths and velocities of stratigraphic units are consistent with the previous results. There is no velocity anomaly observed at well 6B, suggesting a normal stress regime (Figure 13).

Line 5 was deployed with a W-E orientation near line 56 from the August 2012 study. Depths and velocities of stratigraphic units are consistent with the previous results. The velocity

profile from preliminary processing of line 5 data indicated a small anomaly centered on well 4B. The size, geometry, and relative velocity of the anomaly were suggestive of a minor stress buildup in the zone above a void with an undersupported roof. However, subsequent processing with advanced techniques increased the signal-to-noise ratio and significantly improved resolution of the fundamental mode on overtone plots. The final velocity profile has the same general velocity for each layer with less velocity variation within each layer and more laterally coherent stratigraphic contacts (Figure 14). There is a 10-15% velocity increase that begins midway between wells 2B and 4B and increases westward. The geometry and relative velocity of this gentle velocity gradient is suggestive of a natural variation in geology. The small velocity anomaly observed in the preliminary results is likely an indication of the westward velocity gradient, but was poorly resolved due to lack of sufficient signal prior to advanced processing.

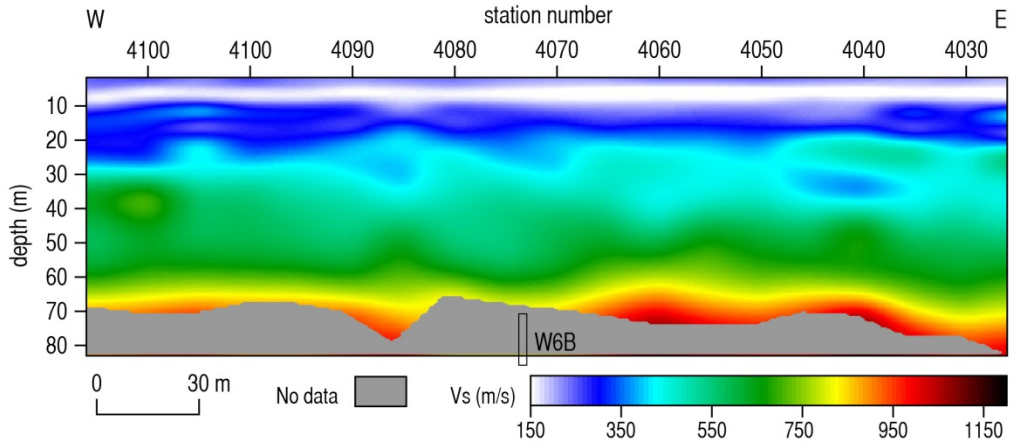

Figure 13. Final shear-wave velocity profile from Line 4 of the October survey. Approximate well locations are indicated at the bottom of the profile.

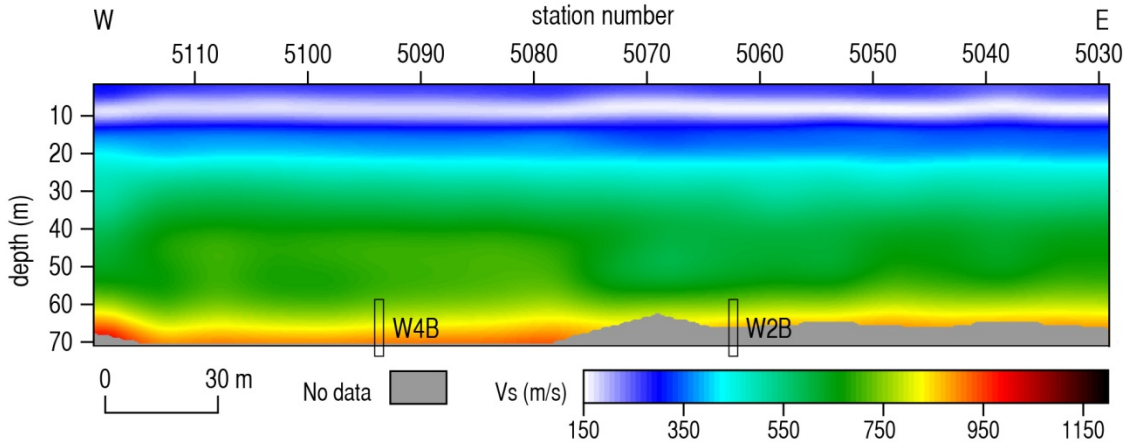

Figure 14. Final shear-wave velocity profile from Line 5 of the October survey. Approximate well locations are indicated at the bottom of the profile.

Line 9 is oriented N-S along William Street. The interpretation of the velocity profile from the preliminary processing of line 9 data suggested gradual natural geologic variation with no signs of elevated shear wave velocity at wells 59, 53, 52, 45, and 17. Due to limited access parallel to William Street the southernmost well intersected by the line was not sufficiently sampled to provide meaningful interpretations of it current status. These results were presented with great caution due to the low signal-to-noise ratio of fundamental mode energy. Subsequent processing with advanced techniques significantly improved the signal-to-noise ratio of fundamental mode energy on overtone plots, and thus increased the confidence in the final results.

Inversion of the updated dispersion curves revealed a similar overall velocity profile with improved lateral coherency of stratigraphic contacts (Figure 15). Bedrock velocities of the northernmost 75 m are representative of those for lines acquired near the Irsik & Doll elevators. Around station 9180, there is a transition to an area with approximately 10-15% higher bedrock velocities, most likely due to a natural variation in geology. A local 5% increase in velocity relative to adjacent stations is observed on and south of well 53, suggestive of a slight increase in stress that does not appear to be significant enough to indicate vertical migration. Considering that the sonar surveys of well 52 and 53 completed several years prior mapped large flat void roofs with no salt cap, these wells have likely continued to undergo incremental collapse. The relatively small increase in shear velocity at well 53 is likely a post-collapse build-up in stress that has followed the failure of that sonar-mapped void roof. Currently, this void likely has a domed roof closer to the ground surface that is gently distributing gradually increasing stress. A 10-15% velocity decrease at well 52, relative to adjacent stations, is indicative of a slight reduction in stress, likely the result of a recent migration event where stress on roof rock was relieved by roof collapse. The velocity structure at wells 17, 45, and 59 appear to be representative of a normal stress regime.

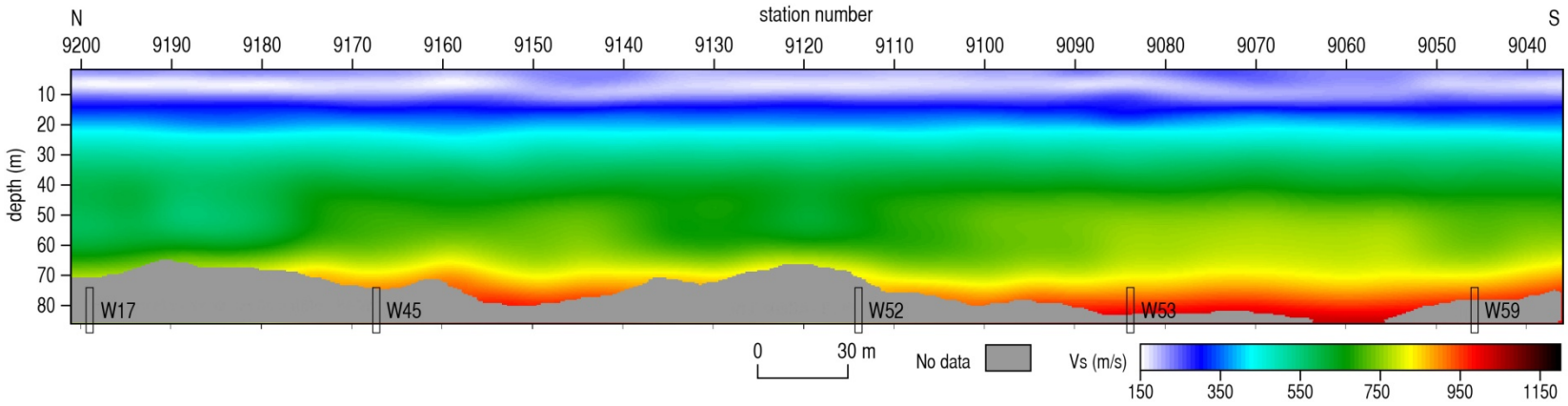

Figure 15. Final shear-wave velocity profile from Line 9 of the October survey. Approximate well locations are indicated at the bottom of the profile.

Study III: Irsik & Doll, wells 2A and 4B follow-up, March 2013

Field Layout and Data Acquisition

A third survey was acquired near the Irsik & Doll elevators to fill in and improve the dataset and enhance the interpretation at wells 2A and 4B. Two 1-D lines and a 2-D grid of receivers were deployed in the study area (Figure 16). As in the previous survey, seismic receivers were single GeoSpace GS11D 4.5 Hz vertical geophones. The 1-D seismic lines varied in length (Table 5), totaling more than 0.5 km with receivers spaced 3 m. The 2-D monitoring grid was deployed with the same receiver spacing and overall layout described above in the Study I field layout section. Data were recorded during one night with a 400+ channel 24-bit Geometrics Geode distributed seismic system. Seismic records were 32 s long with a 2 ms sampling interval. In total, 1060 seismic records equivalent to 21.7 GB of data were recorded.

Figure 16. Aerial photo indicating GPS locations of seismic lines (in orange) and 2D monitoring grid (in yellow) from the March survey, and locations of wells in the study area (yellow pins).

Table 5. Number of receivers and total line lengths for the 1-D seismic lines.

	line 10	line 11
number of receivers	72	115
total length (m)	213	342

Processing and Analysis

Data were processed consistent with the previous surveys, including the use of advanced processing techniques (i.e., time window stacking) applied to sufficiently increase signal-to-noise and improve confidence in final results. The apparent velocity increase associated with source azimuth was less than 5% for the records that were processed (Table 6).

Table 6. Directions of the passive seismic sources and the seismic lines (in degrees counterclockwise from east), the angle of the source with respect to the line (θ), and the percent increase in apparent velocity caused by oblique source orientations (Δv).

line	source orientation	line orientation	θ	Δv
10	350°	1°	11°	2%
11	237°	254°	17°	4.5%

Results and Interpretation

Line 10 was deployed with a W-E orientation directly over well 2A approximately 20 m south of line 1. Line 11 was deployed with a N-S orientation directly over well 2A and approximately 10 m west of well 4B. There is increased depth of surface-wave penetration and a gentle velocity gradient on the west end of the line 10 profile (Figure 17). Stratigraphic layers are relatively flat, and increased depth of surface-wave penetration is observed on line 11 between, but not centered on, wells 2A and 4B (Figure 18). These observations are consistent with results from the other lines acquired over these wells (i.e., lines 1, 56, 5, and 10) and suggestive of natural geologic variation.

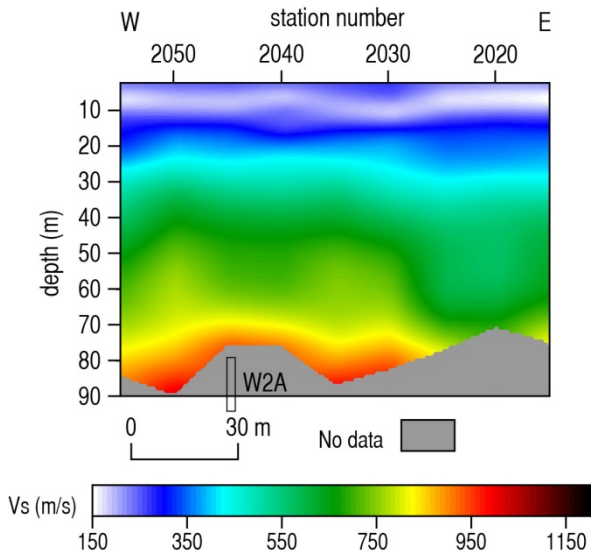

Figure 17. Final shear-wave velocity profile from Line 10 of the March survey. Approximate well location is indicated at the bottom of the profile.

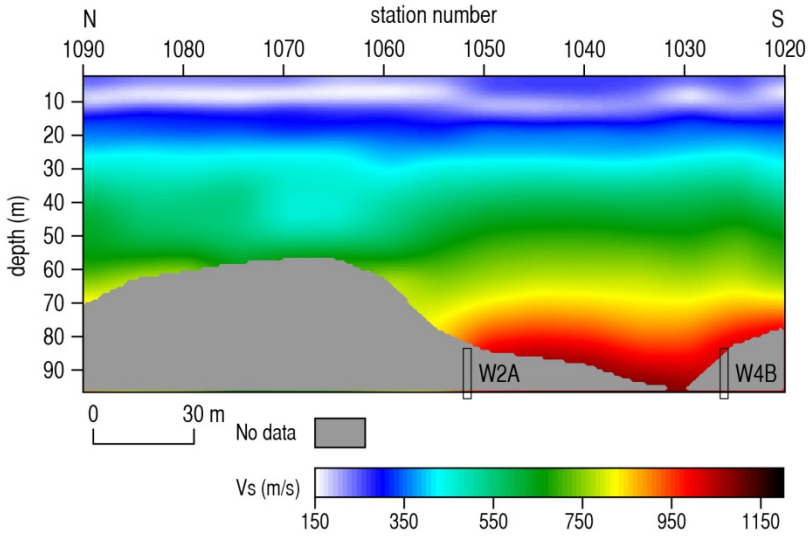

Figure 18. Final shear-wave velocity profile from Line 11 of the March survey. Approximate well locations are indicated at the bottom of the profile.

Comprehensive Interpretation

Well 5B

A velocity anomaly associated with well 5B on line 3 is indicative of a void with a small (<15 m) undersupported roof span (Figure 8). A low velocity anomaly beneath the tensional dome is not observed at the depths imaged, indicating that the void has not migrated above the three finger dolomite. The increase in velocity of the bedrock at well 5B is approximately 15-20%. While this indicates elevated stress, the velocity suggests no failure or reduction of strength at the surface of the bedrock and the threat of failure does not appear to be imminent. This observation on seismic data is consistent with sonar logs taken inside well 5B that were completed in part as a response to and following analysis of these data. Based on the size, geometry, and relative velocity of the tensional dome, this anomaly does not appear to suggest vertical migration.

Wells 2A and 4B

Lines 1, 5, and 10 are oriented W-E and located on either side of the grain elevator. Each of the three lines indicates a gentle westward velocity gradient near wells 2A and 4B (Figures 7, 15, and 18, respectively). The velocity gradient is most likely due to a local, natural variation in geology and suggests little or no increased stress. Line 11 is oriented N-S and crosses the W-E lines near wells 2A and 4B. The increased depth of surface-wave penetration near well 4B (Figure 18) is observed, although to a lesser degree, on line 5 (Figure 14). The observations that stratigraphic layers are relatively flat and that the maximum depth of surface-wave penetration does not occur directly over either well 2A or 4B supports the interpretation that the cause is likely geologic.

There is an off-well anomaly on line 2 (Figure 7) centered approximately 40 m south of well 3B near station 2038, which approximately ties with station 5080 on line 5 (Figure 14). This feature is within the increased velocity zone (discussed above) and about 45 m east of well 4B. This higher-velocity feature is consistent on both lines 2 and 5 and is a subtle indicator of a potential anomaly consistent with a gallery structure.

Wells 1B, 2B, 3B, 6B, 7B, and 12B

Velocity profiles over the remaining wells east of the grain elevators are representative of natural geologic variation and a normal stress regime.

William Street: wells 17, 45, 52, 53, and 59

The velocities observed on line 9 are consistent with an active seismic-reflection survey acquired in 2008 (Miller et al., 2009). A seismic line was acquired at a location equivalent to stations 9040-9135. During the 2008 reflection study, slightly higher shear-wave velocities were observed on this line relative to other lines acquired during the survey. Elevated shear-wave velocity was observed at well 53, where the void was known to have migrated several meters into the shale overburden. A decrease in the velocity of the shale and drop in bedrock and dolomite reflection coherency at well 52 was interpreted as reduction in stress and possible collapse.

Qualitatively, the observations at wells 52 and 53 on line 9 from the October 2012 passive MASW study are relatively consistent with the interpretation of the 2008 active seismic study. These voids have likely undergone incremental collapse, with roof collapse and

subsequent stress reduction followed by a period of gradually increasing stress. A decrease in velocity at well 52 suggests a possibly recent collapse event. A slight increase in velocity at well 53 is suggestive of gradually increasing stress on a domed roof closer to the ground surface than during the previous sonar survey. There does not currently appear to be an imminent threat of vertical migration and collapse. Although the velocities at wells 45 and 59 are slightly greater than those on other lines with no elevated stress, this agrees with the finding from the 2008 survey (Miller et al., 2009) that this line as a whole has slightly greater velocity, most likely due to a natural variation in geology. The velocity profile at well 17 is representative for the site as a whole and indicative of a normal stress regime.

Discussion

The systematic velocity error due to oblique source orientations with respect to the seismic lines is 1-15% for the August survey, <1% for the October survey, and <5% for the March survey. Because the obtained velocity functions are consistent with known geology at this site, the source and line orientations used for these surveys are appropriate. However, error in absolute velocity due to oblique source orientations must be incorporated into the interpretation of the dataset as a whole to avoid attributing increased apparent velocity to increased stress (e.g., line 2). Using equation 2, source orientations of 30° or less will result in a velocity error within the 15% uncertainty inherent to the passive MASW method (Xia et al, 2000).

Line 1 is the nearest line with a W-E orientation to the seismic line from the 2011 passive MASW study (Miller, 2011). The depths to and velocities of the major stratigraphic units are within the 4% error due to the oblique source angle and well within the inherent 15% uncertainty of the passive MASW method. However, the depths obtained with the updated processing algorithm used for these studies are greater than those obtained in the 2011 study. This is consistent with expectations because the inversion algorithm was modified to include the half-space, which provides additional velocity and structural information at the deepest part of each 1-D velocity function in the 2-D profile.

One of the primary differences between the previous and current passive MASW studies is the spread length used for generating overtone images. At this site, longer spreads result in higher amplitude fundamental mode energy on overtone images. The tradeoff is a decrease in spatial resolution inherent with large spreads and increased length of seismic lines. Effectively, long spreads result in lateral “smearing” that may decrease the sensitivity of the method to detect small-scale changes in velocity, thus increasing the amount of data required to image the targets. The 245 m spread length used in the 2011 study was selected because it yielded optimal resolution of fundamental-mode energy on overtone images at the target wavelengths. Spread lengths of only 90-210 m, coupled with the updated inversion algorithm used for the 2012 studies, enabled us to image approximately 30 m deeper with minimal seismic line lengths, thus increasing cost efficiency and depth of investigation.

Conclusions

Velocity information above wells located east of the grain elevator (1B, 2B, 3B, 6B, 7B, and 12B) suggests a normal stress regime. A gentle velocity gradient on the west ends of lines 1 and 5 is suggestive of natural geologic variation, with no obvious anomalous stress associated

with wells 2A or 4B. A dome-shaped increase in velocity centered on well 5B is suggestive of elevated stress on a small, yet undersupported roof. Although the stress is anomalous, it does not appear to be dramatic enough to imply migration or imminent collapse. Voids can be totally benign and possess the observed shear-wave velocity characteristics. Velocities observed at wells 52 and 53 on line 9 are consistent with the 2008 active seismic reflection study (Miller et al., 2009), confirming that passive MASW is an effective tool for evaluating stress above voids of this size and depth. Well 52 has a decrease in velocity that is consistent with a slight reduction in stress, suggesting a recent migration event where stress was relieved by roof collapse. A small decrease in velocity at well 53 is suggestive of post-collapse buildup in stress that followed the failure of the sonar-mapped void roof. Velocities at the remaining wells located along William Street (17, 45, and 59) are suggestive of a normal stress regime.

In general, these results are consistent with 2011 passive MASW study (Miller, 2011). Major stratigraphic units are located at similar depths with consistent velocities. Decreased spread lengths, denser spatial sampling, and inclusion of the half-space during inversion resulted in a more sensitive methodology that provided improved resolution, depth, and cost efficiency. Key to the success of this method is line orientation within 30° with respect to the passive seismic source. This site has excellent passive sources and source orientations ideal for accurate, comprehensive site characterization to depths of 100 m.

Recommendations

Each individual seismic survey can be considered a snap shot in time of the elastic characteristics of the imaged/measured earth. It is well know that as reservoirs, faults, or solution features change over time, so also does their seismic signature. Without a doubt, identifying, interpreting, and quantifying change from several repeat seismic surveys is significantly easier than characterizing features based on a single survey. All the seismic measurements taken as part of this study were analyzed as static in time and without attempting to quantify relative changes between different measurements taken over the period of the study.

To confirm and extend predictions of future surface movement related to void migration, a time-lapse seismic monitoring program should be implemented at this site. Line locations should be coincident with key line locations used during this study. Jugs/voids located within the angle of draw of off-property installations or infrastructure should be the highest priority targets of these surveillance surveys.

Seismic surveying cycles should initially be considered on an annual basis to establish statistical projections and trends. After acquiring three to four surveys during the first few years, statistical trends and associated projections can be confirmed with hard data to use in establishing the cyclicity of future surveys. Based on the consistency and empirically established trend as determined using the initial half-dozen to ten surveys, the need for/value of a longer-term surveillance program can be made and requirements established.

The repeat survey schedule proposed here will allow collection of several data points during the first few years to allow monitoring of void migration rates. These first few surveys will help establish baseline conditions and precision of the method over these particular jugs early in the monitoring period. They will focus on detecting subtle changes in the stress conditions of the area and therefore confirm risk estimates. The repeat surveys will allow statistically confident trend projections and provide early warning to changes in stress conditions, thereby allowing time for more invasive investigations or any remedial action.

References

Dellwig, L.F., 1963, Environment and mechanics of deposition of the Permian Hutchinson Salt Member of the Wellington shale: Symposium on Salt, Northern Ohio Geological Society, p. 74-85.

Dvorkin, J., A. Nur, and C. Chaika, 1996, Stress sensitivity of sandstones: *Geophysics*, v. 61, p. 444-455.

Eberhart-Phillips, D., D.-H. Han, and M.D. Zoback, 1989, Empirical relationships among seismic velocity, effective pressure, porosity, and clay content in sandstone: *Geophysics*, v. 54, p. 82-89.

Holdoway, K.A. 1978, Deposition of evaporites and red beds of the Nippewalla Group, Permian, western Kansas: Kansas Geological Survey Bulletin 215.

Khaksar, A., C.M. Griffiths, and C. McCann, 1999, Compressional- and shear-wave velocities as a function of confining stress in dry sandstones: *Geophysical Prospecting*, v. 47, p. 487-508.

Kulstad, R.O., 1959, Thickness and salt percentage of the Hutchinson salt; in, Symposium on Geophysics in Kansas: Kansas Geological Survey Bulletin 137, p. 241-247.

McGuire, D., and B. Miller, 1989, The utility of single-point seismic data: In Geophysics in Kansas, D.W. Steeples, ed.: Kansas Geological Survey Bulletin 226, p. 1-8.

Merriam, D.F., 1963, The Geologic History of Kansas: Kansas Geological Survey Bulletin 162, 317 p.

Merriam, D.F., and C.J. Mann, 1957, Sinkholes and related geologic features in Kansas: Transactions of the Kansas Academy of Science, v. 60, p. 207-243.

Miller, R.D., 2011, Progress report: 3-D passive surface-wave investigation of solution mining voids in Hutchinson, Kansas: Interim report to Burns & McDonnell Engineering Company, January, 9 p.

Miller, R.D., J. Ivanov, S.D. Sloan, S.L. Walters, B. Leitner, A. Rech, B.A. Wedel, A.R. Wedel, J.M. Anderson, O.M. Metheny, and J.C. Schwarzer, 2009, Shear-wave study above Vig-Industries, Inc. legacy salt jugs in Hutchinson, Kansas: Kansas Geological Survey Open-file Report 2009-3.

Park, C., R. Miller, D. Laflen, N. Cabrillo, J. Ivanov, B. Bennett, and R. Huggins, 2004, Imaging dispersion curves of passive surface waves [Exp. Abs.]: Annual Meeting of the Soc. of Expl. Geophys., Denver, Colorado, October 10-15, p. 1357-1360.

Sayers, C.M., 2004, Monitoring production-induced stress changes using seismic waves [Exp. Abs.]: Annual Meeting of the Soc. of Expl. Geophys., Denver, Colorado, October 10-15, p. 2287-2290.

Sloan, S.D., S.L. Peterie, J. Ivanov, R.D. Miller, and J.R. McKenna, 2010, Void detection using near-surface seismic methods; *in* Advances in Near-Surface Seismology and Ground-Penetrating Radar, SEG Geophysical Developments Series No. 15, R.D. Miller, J.D. Bradford, and K. Holliger, eds.: Tulsa, Society of Exploration Geophysicists, p. 201-218.

Swineford, A., 1955, Petrography of upper Permian rocks in south-central Kansas: State Geological Survey of Kansas Bulletin 111, 179 p.

Walters, R.F., 1978, Land subsidence in central Kansas related to salt dissolution: Kansas Geological Survey Bulletin 214, 82 p.

Xia, J., R.C. Miller, C.B. Park, J.A. Hunter, J.B. Harris, 2000, Comparing Shear-Wave Velocity Profiles from MASW with Borehole Measurements in Unconsolidated Sediments, Fraser River Delta, B.C., Canada: *Journal of Environmental and Engineering Geophysics*, v. 5, p. 1-13.